PCCP

Accepted Manuscript

ROYAL SOCIETY OF CHEMISTRY

www.rsc.org/pccp

Journal Name

RSCPublishing

ARTICLE

Thermotropic cubic and tetragonal phases made of rod-like molecules†

Cite this: DOI: 10.1039/x0xx00000x

M. Vogrin[a], N. Vaupotič[a,b], M. Wojcik[c], J. Mieczkowski[c], K. Madrak[c], D. Pociecha[c,*], E. Gorecka[c]

Received 00th January 2012,
Accepted 00th January 2012

DOI: 10.1039/x0xx00000x

www.rsc.org/

Systematic studies of three dimensionally ordered liquid crystalline phases of different cubic and tetragonal symmetries are presented. Structures of the phases are determined by a reconstruction of the electron density distribution from the X-ray diffraction patterns. The known models for electron densities in cubic structures were used whereas a new theoretical model for the structure of the tetragonal phase, which gives good agreement with the experimentally obtained electron densities, was proposed. For the first time a continuous phase transition between three dimensional phases with tetragonal and monoclinic symmetries was observed for optically pure compound.

Introduction

Thermotropic liquid crystalline cubic phases are three-dimensionally (3D) ordered, highly symmetric structures, which can be formed also by strongly anisotropic mesogenic molecules. They are relatively common among the rod-like, polycatenar, polyhydroxy and dendritic molecules (see, for example, the overview papers by Tschierske and Diele and the references therein[1,2,3]). The bicontinuous cubic phases can be considered as made of channels filled with aromatic parts of molecules, separated by space filled with alkyl tails; in channels molecules display only short range positional correlations. A crystallographic unit cell of cubic phase contains hundreds of molecules. Different types of cubic phases have been observed, depending on the spatial arrangement and interconnections of the channels. The most common is a double gyroid structure with the *Ia*3*d* symmetry, while the tri-continuous cubic phase with the *Im*3*m* symmetry is less frequent. A single gyroid cubic structure with the $I4_132$ symmetry has been observed[4,5,6]. Even less common are tetragonal 3D liquid crystalline phases, so far observed in few materials. Tetragonal phase was first reported in 1983[7] and called the SmQ phase. The structure has later been identified as a tetragonal twist grain boundary (TGB)[8] in which lattice of dislocations is three-dimensional, as opposed to the commonly known smectic TGB phases, having blocks of layers separated by parallel walls containing defects. There are, in general, three types of tetragonal LC phases, labelled: T*I, T*II and T*III, having the *I*422, $I4_122$ and $P4_122$ space group symmetry, respectively[8,9]. The T*II phase is often called a bi-continuous tetragonal phase.

It is assumed that the 3D density modulated phases are made from strongly distorted smectic layers or columns, depending on the type of constituent molecules. For thermotropic materials transitions from the lamellar to the cubic gyroid phase[10,11,12] and from the hexagonal columnar to the cubic gyroid phase[13,14] were found and a morphological evolution from the double gyroid (*Ia*3*d*) to the lamellar and columnar hexagonal phase was studied[15]. An evidence of a phase transition from the hexagonal columnar to the cubic phase with the *Im*3*m* symmetry was also given[16,17]. In addition, several systems showing transitions between different 3D phases are known, for example: from the cubic double gyroid (*Ia*3*d*) to the tri-continuous cubic (*Im*3*m* symmetry)[11,12,18] and from the cubic double gyroid (*Ia*3*d* symmetry) to the bi-continuous tetragonal phase ($I4_122$ symmetry)[19]. In some systems the tetragonal gyroid phase was observed as a path between the cubic double gyroid (*Ia*3*d* symmetry) and the tri-continuous cubic (*Im*3*m* symmetry) phases[20,21].

Formation of the 3D phases is very sensitive to molecular factors, e.g. even small changes in the length of terminal chains might have a crucial effect on the behavior of the system. For homologues with alkyl chains which are long enough a phase sequence Cry → lamellar SmC → cubic (*Im*3*m*) → cubic (*Ia*3*d*) → tetragonal phase was reported, while for shorter alkyl chains a common phase sequence Cry → SmC → SmA → Iso was observed[12]. Few authors pointed out that the type of a 3D structure might be influenced by chirality of the system. Yamamoto *et. al.*[9] have studied a binary phase diagram for dichiral azobenzene compounds as a function of chirality and temperature. In racemic mixtures the phase sequence Cry → cubic (*Im*3*m*) → Iso was observed upon heating. By increasing the optical purity (increasing concentration of either the (S,S) or (R,R) isomers) the cubic structure with the *Im*3*m* symmetry transforms into a chiral cubic structure with the *I*432 symmetry.

Further increase of optical purity led to the formation of a tetragonal (T*I or T*II) structure.

Identification of the symmetry of the cubic or tetragonal phase is usually straightforward from the X-ray diffraction pattern. On the other hand, revealing the internal structure of crystallographic unit cell is an intriguing task. It could be done by the reconstruction of the electron density map through the reverse Fourier transform of the X-ray pattern, however in a standard X-ray experiment only information related to the amplitude of structure factor (related to the square root of signal intensity) is available, while the information about the structure factor phase is lost. Moreover, for cubic phases multiplicity of signals is high and peaks belonging to the same multiplicity set might have different phases. One way to solve this problem is to construct a model of a 3D electron density distribution and calculate its Fourier transform. An appropriate model should yield the signal amplitude ratios close to the experimental ones. Finally, the electron density map is reconstructed using experimental amplitudes and theoretically obtained phases. Usually it is enough to use only few signals of the highest intensity, as the other peaks do not affect the electron density significantly. For a double gyroid cubic phase (*Ia3d* symmetry), which has been studied theoretically most extensively[22,23,24,25], two highest intensity peaks are (211) and (220). For the cubic single gyroid structure ($I4_132$) the dominant signal is (110)[4,6] and in the tri-continuous cubic phase (*Im3m*) the strongest peaks are (321) and (400)[26,27,28].

While an extensive effort, both experimental and theoretical, was devoted to reproduce electron density maps of cubic phases, there are only few reports on tetragonal liquid crystalline phases. Infinite periodic minimal surface model (IPMS) of a tetragonal gyroid structure has been proposed[20,21]. The models for the 3D TGB phases (T*I,II,III) have been proposed[8], however no direct comparison between theoretically predicted and experimentally observed X-ray diffraction patterns were given.

In this paper we report on detailed X-ray diffraction studies that enabled a reconstruction of the electron density distribution in cubic as well as, for the first time, in tetragonal LC phases. Systematic studies of the effect of chirality, optical purity, length of terminal chains and their branching on the 3D packing of rod-like mesogenic molecules were conducted.

Results

The constituent molecules of all the studied materials (denoted by ***n/k***, see Fig. 1) have the same, symmetric 4,4'-bis(4''-carboxybenzyloxy)biphenyl mesogenic core.

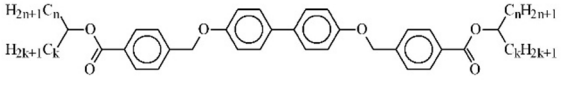

Figure 1. Molecular structure of the studied compounds ***n/k*** (4,4'-bis(4''-carboxybenzyloxy)biphenyl derivatives).

They differ in the type, length and branching of terminal chains. The general synthetic route is outlined in Scheme 1, for details see ESI. The phase transition temperatures and associated transition enthalpies are shown in Table 1, results from both, heating and cooling, scans are shown as in some cases observed phase sequence depend on a sample history. The majority of the studied materials is racemic, however, in the case of the compound **6/1** stereoisomers with absolute **R/R** (pure enantiomer) and **R/SR** (partially racemized) or **RS/RS** (racemic mixture) configurations of two chiral centers were prepared in order to study the influence of optical purity on the structure formed.

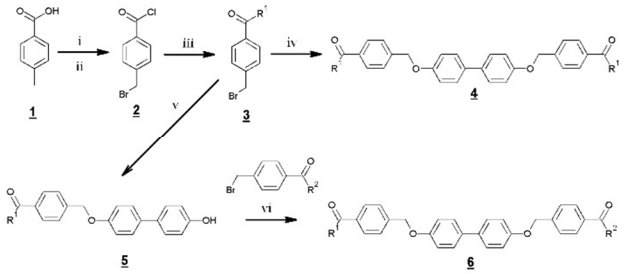

Scheme 1. Synthetic route for studied compounds: **4** (all, except **6/1 (R/RS)** and **6** (**6/1 (R/RS)**). Reaction conditions: i) Br2, hv; ii) SOCl2, CHCl3, reflux; iii) R1OH, pyridine, toluene; iv) KI, K2CO3, 4,-4' – dihydroxybiphenol (0,5 eq), DMF; v) KI, K2CO3, 4,-4' – dihydroxybiphenol (2,5 eq), DMF; vi) KI, K2CO3, excess of alkyl 4-(bromomethyl)benzoate , DMF.

Table 1. The phase transition temperatures and associated enthalpies for the studied mesogens, determined by DSC on heating and cooling scans.

Compound **n/k**	Phase sequence [a]
6/1 (RS/RS)	Cr 100.0 (30.5) SmC_A 132.9 (2.0) Cub_1 148.0 (19.7) Iso Iso 145.7 Iso_1 143.5 (17.8[b]) SmC_A 140.4 (1.8[c]) Cub_1 107.8 (3.8) SmC_A 86.6 (23.2) Cr
6/1 (R/RS)	Cr 108.7 (37.2) SmC 137.1 (2.1) Cub_1 144.6 Iso_1 148.4 (20.4[b]) Iso Iso 147.1 (13.4) Iso_1 138.2 (5.2) Cub_1 101.0 (32.6) Cr
6/1 (R/R)	Cr 125.2 (45.0) SmC_A 130.7 (3.3) M 137[d] T 142.6 (3.6) Iso_1 150.1 (11.9) Iso Iso 149.0 (13.5) Iso_1 138.4 (2.1) M 131[d] T 122.6 (3.9) SmC_A 114.9 (42.9) Cr
9/1 (RS/RS)	Cr 86.7 (40.6) Cub_1 125.9 (13.4) Iso Iso 125.4 (11.8) Cub_1 70.1 (23.6) Cr
10/1 (RS/RS)	Cr 108.3 (47.9) Cub_1 133.3 (16.9) Iso Iso 130.4 (16.1) Cub_1 78.1 (26.9) Cr
9/2 (RS/RS)	Cr 56.9 (27.8) Cub_2 94.4 Iso_1 101.2 (10.0[b]) Iso Iso 99.2 Iso_1 92.4 (11.2[b]) Col_h / Cub_2
4/4	Cr 93.7 (48.1) Cub_1 121.6 (7.3) Iso Iso 118.9 (10.9) Cub_1 71.0 (21.7) Cr

[a] Cr – crystal, Cub_1 – *Ia3d*, Cub_2 – *Im3m*, M – monoclinic *I*112, T – tetragonal $I4_122$, Col_h – columnar hexagonal (2D), Iso_1 – isotropic phase with short-range ordered structure (most probably sponge-type cubic phase) , Iso – isotropic liquid; [b] total enthalpy, [c] endothermic signal on cooling scan, [d] from X-ray diffraction experiments

For a fully racemic compound **6/1 (RS/RS)** a phase transition from the anticlinic smectic SmC_A to the cubic phase was found on heating. In optical microscopy studies (crossed polarizers setup) the first order transition from the SmC_A phase to the cubic phase is observed as a sudden disappearance of birefringence. The dark areas of cubic phase growing from the SmC_A phase have straight, sharp boundaries. Interestingly, on a cooling run, the SmC_A phase appears twice in the phase sequence: it is observed in a narrow temperature range between the isotropic liquid and cubic phase as a metastable state, and again it is formed as a stable state below the cubic phase (Fig. 2). The X-ray diffraction studies confirmed a lamellar structure of the SmC_A phase, with the layer thickness close to 3.1 nm, much shorter than the length of a fully stretched molecule (~4.3 nm), indicating large molecular tilt (~43 deg). In the cubic phase, the best indexing of the X-ray pattern was obtained for the double gyroid, *Ia3d*, symmetry with the lattice parameter a = 8.35 nm (Fig. 3). While the racemic compound **6/1 (RS/RS)** forms cubic phase, in its optically pure analogue, compound **6/1 (R/R)**, the SmC_A phase transforms on heating to a phase showing weakly birefringent, plate-like texture, which excludes the cubic symmetry.

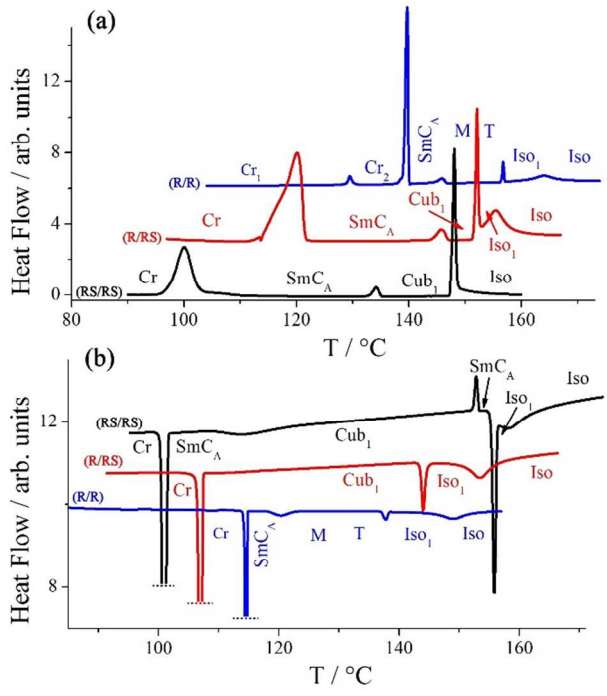

Figure 2. DSC thermograms for compounds **6/1** obtained on (a) heating and (b) cooling scans. Lines are shifted (vertically and horizontally) for clarity of presentation. Iso_1 stands for isotropic liquid with short range ordered structures, most probably resembling a sponge type cubic phase.

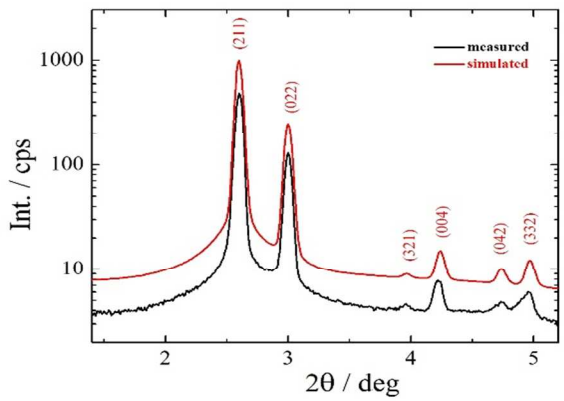

Figure 3. X-ray patterns for cubic phase of compound **6/1** (**RS/RS**): (black) measured and (red) simulated assuming the double gyroid *Ia3d* symmetry with the lattice parameter a = 8.35 nm. Simulated curve is vertically shifted for clarity.

X-ray diffraction studies reveal a sequence of two 3D phases above the smectic phase (Fig. 4), transition between them is not accompanied by a measurable enthalpy change. The phases are identified as monoclinic (*I*112 or *I*112/m) and tetragonal ($I4_122$). Their structures are closely related, the crystallographic unit cell dimensions do not change at the phase transition, only the angle γ between the $\vec{a}$ and $\vec{b}$ base vectors, which is 90 deg in the tetragonal phase, deviates by up to 7 deg in the monoclinic phase (inset in Fig. 4). Thus the monoclinic structure might be considered as slightly distorted tetragonal one. Because a continuous change of the angle γ with temperature is observed, the transition between the monoclinic and tetragonal phases is of the second order. Under an electric field one observes the first order phase transition of the 3D phases into the lamellar SmC phase.

The volumes of crystallographic unit cells for cubic phase of compound **6/1 (RS/RS)** and tetragonal and monoclinic phases of compound **6/1 (R/R)** are similar – they all contain about 550 molecules.

Racemization of one chiral center – in compound **6/1 (RS/R)** - re-induces the cubic *Ia3d* phase, with lattice parameter similar to the one observed in the fully racemized analogue. However, in thin glass cells (thicknesses below 2 microns) filled with compound **6/1 (RS/R)** a weakly birefringent plate-like regions that can be ascribed to either monoclinic or tetragonal structures, were also observed. The cubic phase with the *Ia3d* symmetry was also found for fully racemic homologues **9/1** and **10/1**. The lattice parameter changed monotonically with elongation of terminal chains, being 8.46 nm for **6/1**, 9.24 nm for **9/1**, and 9.35 nm for **10/1** compounds. Assuming the same density of all materials, the number of molecules (~550) in the unit cell remained independent on the homologue, showing that changing the size of molecules affects mainly the volume of those regions in the unit cell, which are filled by alkyl chains.

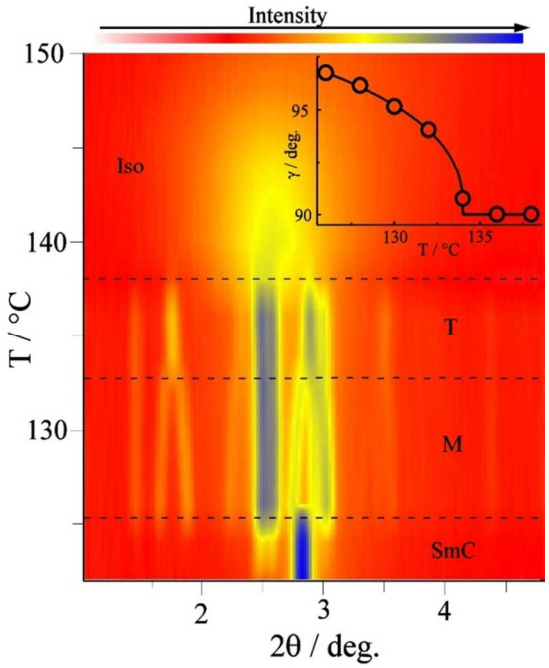

Figure 4. Temperature evolution of the X-ray diffraction pattern, observed on cooling, for compound **6/1 (R/R)**, the intensity of the signals is coded with colour. In the inset the temperature dependence of the angle γ between base vectors of crystallographic unit cell, close to the phase transition from the tetragonal (T) to the monoclinic (M) phase.

The branching of molecular tails has an interesting influence on the phase stability. For compound **9/2 (RS/RS)** a different phase sequence is observed on heating and on cooling scans. Upon heating from the crystalline phase, the material has a tendency to form large domains of cubic phase, which melt directly to an isotropic liquid. Upon cooling from the isotropic phase, a birefringent texture characteristic for a columnar phase is detected. The X-ray measurements indicate hexagonal symmetry of columns with lattice parameter a = 3.95 nm (Fig. 5). The columnar phase undergoes a transition to cubic phase not only by lowering the temperature, but also with time, which proves its metastable nature. For the cubic phase the best fit to the experimentally observed signals was obtained assuming either the *Im*3*m* or *I*432 symmetry, with a = 13.0 nm (Fig. 6).

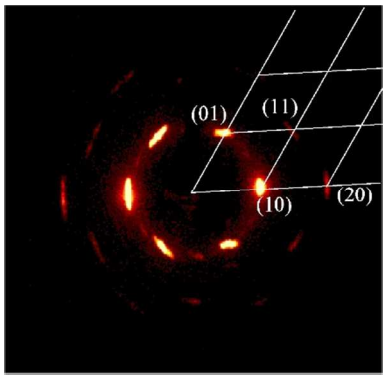

Figure 5. Small angle X-ray diffraction pattern of an aligned sample of compound **9/2** in the columnar phase, showing the six-fold symmetry of the structure.

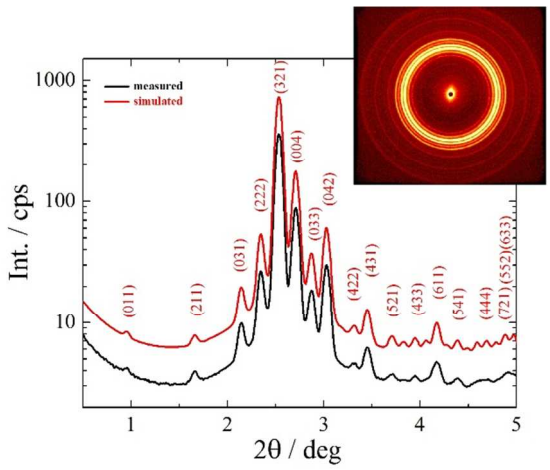

Figure 6. The X-ray diffraction patterns for the cubic phase of compound **9/2**: (black) measured and (red) simulated assuming either the *I*432 or *Im*3*m* symmetry with lattice parameter a = 13.0 nm. In the inset: 2D X-ray diffraction pattern of a powder sample in the cubic phase.

For compound **4/4** a double gyroid cubic phase (*Ia*3*d* symmetry, lattice parameter a = 9.24 nm) was found.

In all the phases, with 1D, 2D and 3D ordered structures, a diffused signal was detected in the high angle region of the X-ray pattern (corresponding to 0.45 nm distance) that is typical for the short range positional order inside layers, columns or channels.

For some materials having a transition from an isotropic liquid to a 3D ordered phase, a broad signal was found in calorimetric studies, a few degrees above the clearing temperature (Fig. 2), with related thermal effect up to 14 Jg^{-1} (for **6/1 (R/R)**). In this range the X-ray measurements show single, intense, but diffused signal in the low angle region (see Fig. 4). These observations suggest existence of some short range ordered structures, most probably resembling a sponge type cubic or tetragonal phase. The stability of the sponge type phase strongly depends on the optical purity of the material, the widest temperature range, up to 10 K, was observed for pure enantiomer **6/1 (R/R)**.

Electron density reconstructions

The electron density $\rho(x,y,z)$ is reconstructed from the experimentally measured amplitudes and positions of the X-ray diffraction peaks. The position of the peak is defined by the wave vector $\vec{q}$ in the reciprocal lattice. In the cubic structure $\vec{q} = 2\pi(h/a, k/a, l/a)$ and in the tetragonal lattice $\vec{q} = 2\pi(h/a, k/a, l/c)$, where (hkl) are the Miller indices. The electron density map can be produced by the reverse Fourier transform as:

$$\rho(x,y,z) = \sum_{hkl} |F|_{hkl} \cos(\vec{q} \cdot \vec{r} + \phi_{hkl}) \qquad (1)$$

Thus, to reconstruct the electron density, one needs the information on the amplitude ($|F|_{hkl}$) and the phase (ϕ_{hkl}) of each (hkl) signal. However, the X-ray diffraction measurements give information only on the amplitudes of the peaks; the information on the phase is lost. In highly symmetric structures one can guess the phases to be either 0 or π and then check all the possible structures and decide which is the most probable one. However, it is more appropriate to construct an electron density model, calculate its Fourier transform and obtain theoretical values for the amplitudes and phases. The model is optimized to yield comparable ratios between signal amplitudes as detected in experiment. Theoretically obtained phases of signals are then used to reconstruct the electron density maps from experimentally obtained amplitudes.

For the double gyroid (*Ia*3*d*) structure, which was observed for racemic **(RS/RS)** compounds **6/1**, **9/1**, **10/1**, **4/4** and for compound **6/1 (R/RS),** the theoretical model is known, amplitudes and phases of the diffraction peaks have already been calculated[22,23,24,25]. Table 2 gives the theoretical ($|F|_{hkl}^{th}$) and experimental ($|F|_{hkl}^{exp}$) amplitudes for (hkl) peaks detected experimentally as well as theoretical values of phases (ϕ_{hkl}^{th}). In cubic structures, each (hkl) peak has the same amplitude for all the possible permutations of *h, k* and *l*, however their phases might be different, but can be determined from the crystallographic tables[299] if the phase of one peak is known, so we give the phases only for a particular (hkl) combination given in the left column in the table. The electron density map calculated from the X-ray pattern of the compound **6/1 (RS/RS)** is presented in Fig. 7a.

Table 2. Theoretical amplitudes[23] $|F|_{hkl}^{th}$ and phases ϕ_{hkl}^{th} and experimental amplitudes ($|F|_{hkl}^{exp}$) measured for compound **6/1 (RS/RS)**; the *Ia*3*d* symmetry was used for indexing the peaks.

hkl	ϕ_{hkl}^{th}	$\lvert F\rvert_{hkl}^{th}$	$\lvert F\rvert_{hkl}^{exp}$
211	0	1	1
220	0	0.6808	0.7113
400	π	0.5467	0.7106
420	π	0.5119	0.0588
332	0	0.707	0.0820

For some compounds it was found that, on cooling, the cubic double gyroid phase undergoes a phase transition into the lamellar (smectic C_A) phase. It was suggested[30] that the phase transition takes place by the epitaxial matching of the spacing of smectic layers and (220) planes of cubic (*Ia*3*d*) phase. Fig. 7b shows the cross-section of the obtained electron density map in the (220) plane, to visualize the planes where the smectic layers can attach, molecules are added to the figure. In the SmC_A phase the tilt of the molecules in the neighboring layers is in the opposite direction and it is close to 45 deg. This anticlinic tilt determines the orientation of molecules in the channels of the double gyroid cubic phase, as shown in Fig. 7.

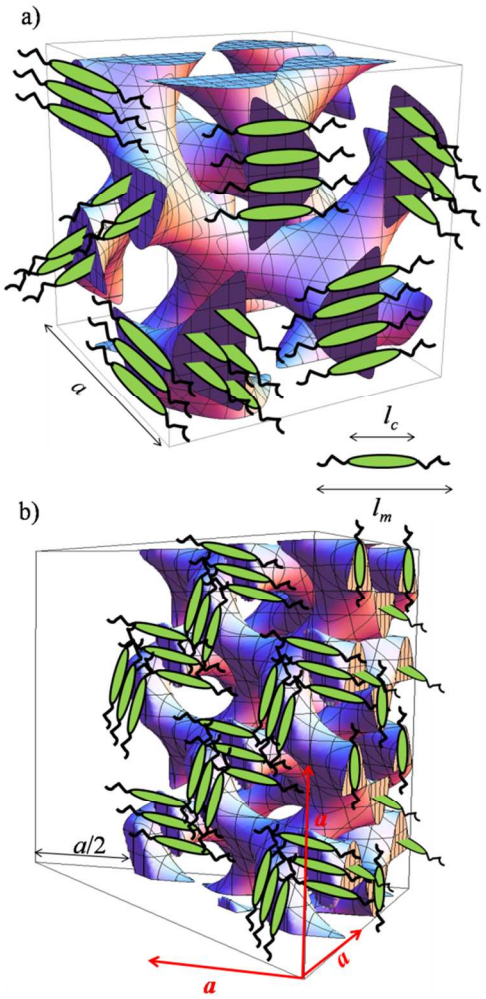

Figure 7. a) Experimentally obtained electron density map for one unit cell of cubic double gyroid structure (*Ia*3*d* symmetry) of material **6/1 (RS/RS);** a = 8.46 nm, l_m = 4.3 nm and l_c = 2.5 nm. b) The (220) cross-section of the double gyroid cubic structure. The orientation of the molecules in the channels of the double gyroid cubic structure is determined by the lower temperature lamellar smectic C phase with the anticlinic tilt of molecules in the neighboring layers.

In optically pure compound **6/1 (R/R)**, the phase with tetragonal symmetry was detected. Since no theoretical calculations of the structure factor amplitudes and phases for tetragonal LC phases are available, a simple model of the T*II phase ($I4_122$ symmetry) was constructed. The idea for the model was obtained from the structure suggested by Pansu *et al.*[31] in which crystallographic unit cell consists of 8 molecular blocks (Fig. 8a) arranged into four levels; the blocks rotate by $\pi/4$ from one level to the other (Fig. 8b). Inside one level there are two blocks which are tilted in the opposite direction, defining the opposite tilt of the molecules in these neighboring blocks. The length of the blocks is equal to the length of the unit cell, a, but their width and height are lower than one half of the width and one eight of the height of the unit cell, respectively. The electron density inside the block is assumed constant and equal in all blocks, while outside of the blocks the density is set to zero. Fourier transform of such an electron

density distribution gives the amplitudes and phases of the XRD peaks.

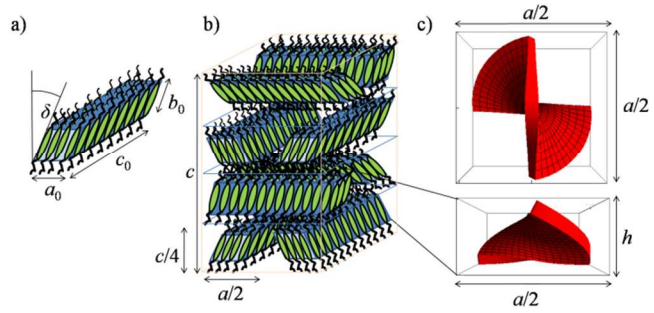

Figure 8. The block model of the tetragonal T*II phase ($I4_122$ symmetry). The constituent blocks (a) are arranged into four levels (b). Inside one level there are two blocks which are tilted in the opposite direction. The blocks rotate by $\pi/4$ from one level to the other and are connected by helicoidally twisted layers (the top and the side view are given) which have lower density than the main blocks (c).

The amplitudes are very sensitive to the chosen values of parameters a_0, b_0, c_0 and δ (Fig. 8a). The model predicts the highest amplitudes for the same peaks: (020), (004) and (013), as observed experimentally. However, it predicts zero intensity for the (211) and (110) peaks, which disagrees with the experiment.To account for these peaks the model was upgraded by adding regions of helicoidally twisted electron density between the neighboring levels (Fig. 8c). From the size of the unit cell one can infer that the main blocks (blue) contain only one layer of molecules and that the helical connecting regions (red) contain mainly the tails of the molecules from the top and bottom blocks. Thus the electron density in the connecting regions was set to be lower than in the main blocks. The amplitudes and phases obtained at a chosen set of parameters a_0, b_0, c_0 and δ are given in Table 3. Due to the tetragonal $I4_122$ symmetry, the signal phases are not only 0 or π anymore. Moreover, one has to keep in mind that the amplitudes are the same for all permutations of h and k in the (hkl) peak, but the phases might be different. Table 3 gives also the experimentally obtained amplitudes for the highest intensity peaks, from which the electron density is reconstructed, by using eq. (1) (Fig. 9).

Table 3. Theoretical amplitudes ($|F|^{th}_{hkl}$) and phases (ϕ^{th}_{hkl}) and experimental amplitudes ($|F|^{exp}_{hkl}$) measured for the **6/1 (R/R)** material; a tetragonal $I4_122$ symmetry was used for indexing the peaks. Parameter values: $a_0 = 0.25a$, $b_0 = 0.74\ c/4$, $c_0 = a$, $\delta = 0.93\ \pi/2$, and $c = 1.65\ a$. The electron density in the helically twisted connecting blocks was chosen as 1/3 of the electron density in the main blocks.

hkl	ϕ^{th}_{hkl}	$\|F\|^{th}_{hkl}$	$\|F\|^{exp}_{hkl}$
020	π	1	1
004	π	0.6576	0.6459
013	-0.22 π	0.6589	0.6322
211	π	0.2467	0.3571
110	π	0.3874	0.3309
022	$\pi/2$	0.5978	0.3058

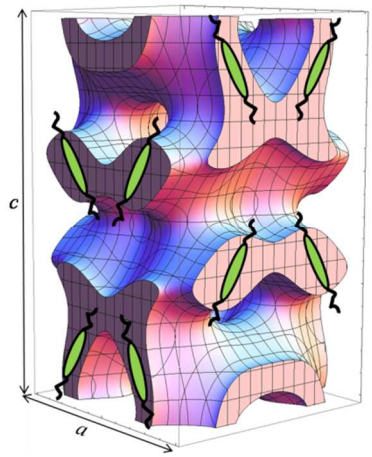

Figure 9. The electron density map of one unit cell of the tetragonal phase T*II with the $I4_122$ symmetry obtained from the experimental amplitudes (see Table 3) and theoretical phases using the highest 6 peaks (013), (004), (020), (110), (211), (022). In each block one molecule is drawn in order to visualize the orientation of molecules in the block (compare also with Fig. 1). a = 7.1 nm, c = 1.65 a.

Finally, the electron density map for cubic phase of compound **9/2** was obtained, which exhibits a phase transition from columnar hexagonal to cubic structure. Several X-ray diffraction peaks are observed for the cubic phase that can be indexed assuming either the $I432$ chiral or $Im3m$ achiral tri-continuous structure. Since the studied material is racemic we assume the $Im3m$ symmetry. A theoretical model of the $Im3m$ symmetry structure has already been proposed[26-28]. We have constructed electron density maps with several phase combinations and find that the electron density maps change significanty only by changing the phases of the (400) and (321) peaks, as already argued by Ozawa *et al*[28]. The theoretical and experimental amplitudes and phases are given in Table 4 and the corresponding electron density maps, following from the experimental amplitudes and theoretical phases, are given in Fig. 10.

Table 4. Theoretical amplitudes ($|F|^{th}_{hkl}$) and phases (ϕ^{th}_{hkl}) (obtained from ref. 26) and experimental amplitudes ($|F|^{exp}_{hkl}$) measured for compound **9/2**; the $Im3m$ symmetry was used to index the peaks.

hkl	ϕ^{th}_{hkl}[26]	ϕ^{th}_{hkl}[31]	$\|F\|^{th}_{hkl}$ [26]	$\|F\|^{exp}_{hkl}$
400	0	π	0.9252	1
321	π	π	1	0.7374
222	0	0	0.0776	0.4342
420	0	0	0.5530	0.2837

For the $Im3m \rightarrow Col_h$ transition, Zhu *et al.*[17] predicted the following planes where columns can attach to the channels in the tri-continuous cubic phase: $Hex[001] \rightarrow Im3m[222]$, $Hex[100] \rightarrow Im3m[121]$, and $Hex[120] \rightarrow Im3m[101]$. The X-ray analysis shows that the periodicity related to the (321) peak of the cubic $Im3m$ phase is very close to the periodicity of the (100) peak in the hexagonal phase.

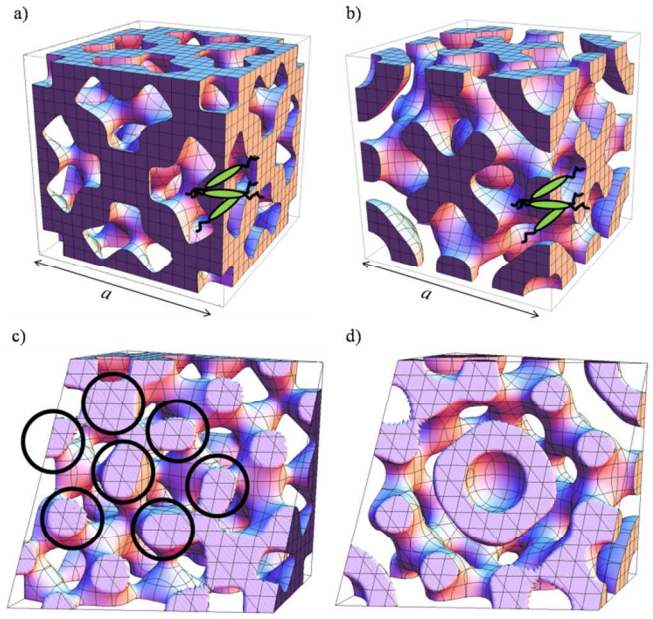

Figure 10. Experimental electron density map of one unit cell of material **9/2** assuming the cubic *Im*3*m* symmetry with a) (0,π) and b) (π,π) phase combinations for the two highest peaks. The (400), (321), (222) and (420) peaks were used for the reconstruction (see Table 4). Molecules are oriented perpendicular to the channels. The length of the unit cell (a = 13.0 nm) approximately equals to three molecular lengths. c) A cut of the structure along the (211) plane for the (0,π) phase combination for the two highest peaks and d) A cut of the structure along the (211) plane for the (π,π) phase combination for the two highest peaks. In c) circles mark positions where the columns of the Col_h phase can attach. We were not able to find such a correspondence for the (π,π) phase combination for the two highest peaks since the inner channel network[27] is not present in this case.

Among the planes, suggested by Zhu, the planes (211) and (222) are perpendicular to the (321) plane. In these two planes one should thus search for the possibility for the columns to attach. A cross-section of the electron density map reconstructed with the (0,π) phase combination along the (211) plane gives clear positions where the attachment is possible, as shown in Fig. 10c, while we could not find such correspondence in the (222) plane. With the phase combination (π,π) we could not find a correspondence in any plane. In Fig. 10d we thus give the same cross-sections for both structures in order to show the difference.

Conclusions

Variety of 3D ordered structures were found for thermotropic liquid crystals formed by symmetric rod-like molecules with two chirality centers. Racemic mixtures, in general, exhibit double gyroid cubic phases (*Ia*3*d* symmetry) and lamellar anticlinic SmC_A phase at lower temperatures. An increase in branching of terminal chains stabilizes the tri-continuous cubic phase (*Im*3*m* symmetry), which compete with metastable columnar hexagonal (2D) phase. This suggests that cubic *Ia*3*d* and *Im*3*m* phases have different origins, the first one can be considered as made of strongly distorted layers while the later as built of distorted columns. Increase in optical purity results in formation of a phase with a tetragonal unit cell and the $I4_122$ symmetry. To obtain the distribution of molecules in the tetragonal phase, a model was proposed in which molecules are arranged into tilted blocks; one unit cell consists of 4 levels of blocks which rotate by $\pi/2$ from one level to the other. In order to fully account for the observed X-ray diffraction pattern, helicoidally twisted connections between blocks had to be added.

Upon lowering temperature, for the first time a continuous phase transition between two 3D phases with tetragonal and monoclinic structures was observed. The transition takes place by a subtle distortion of a tetragonal lattice, during which its base changes from a square into a rhomb.

Finally, it was observed that for non-fully racemized materials the external electric field stimulates the irreversible transition from the cubic or tetragonal phase to the lamellar smectic phase with anticlinic arrangement of molecules in the neighboring layers.

Experimental

Phase transition temperatures and their thermal effects were determined with Perkin Elmer DSC-7 calorimeter, samples of mass 1-3 mg were sealed in aluminum pans and kept in nitrogen atmosphere during measurement; both heating and cooling scans with rate 5-10 K/min were applied.

The X-ray diffraction patterns in small angle range were obtained with the Bruker Nanostar system (CuK_α radiation, cross-coupled Goebel mirrors, area detector VANTEC2000) for the powder as well as partially aligned samples. The temperature of the sample was controlled with precision of 0.1 K. Samples were prepared either in thin-walled glass capillaries or as droplets on heated surface. Wide angle diffractograms were obtained with Bruker D8 GADDS system (CuK_α line, Goebel mirror, point beam collimator, Vantec2000 area detector).

The optical studies were performed using Zeiss Imager A2m polarizing microscope equipped with Linkam heating stage.

Acknowledgements

MV and NV acknowledge the financial support of the ARRS research program P1-0055. The work was supported by the NCN grant no. 2012/07/B/ST5/02448.

Notes and references

[a] Faculty of Natural Sciences and Mathematics, University of Maribor, Koroška 160, Maribor, Slovenia.

[b] Jozef Stefan Institute, Jamova 39, 1000 Ljubljana, Slovenia.

[c] Department of Chemistry, University of Warsaw, Al. Żwirki i Wigury 101, 02-089 Warsaw, Poland.

† Electronic supplementary information (ESI) available: Synthesis and spectral characterization of studied compounds. See DOI: 10.1039/c4cp01310g

1. C. Tschierske, *Angew. Chem. Int. Ed*, 2013, **52**, 8828-8878.

2. S. Diele, *Current opinion in colloid & interface science*, 2002, **7**, 333-342.
3. C. Tschierske, *Current opinion in colloid & interface science*, 2002, **7**, 69-80.
4. M. Seki, J. Suzuki and Y. Matsushita, *J. Appl. Cryst.*, 2000, **33**, 285-290.
5. K. Michielsen and D. Stavenga, *J. R. Soc. Interface*, 2008, **5**, 85-94.
6. V. Saranathan, C. O. Osuji, S. G. Mochrie, H. Noh, S. Narayanan, A. Sandy, E. R. Dufresne and R. O. Prum, *Proceedings of the National Academy of Sciences*, 2010, **107**, 11676-11681.
7. A. Levelut, C. Germain, P. Keller, L. Liebert and J. Billard, *J. Phys.*, 1983, **44**, 623-629.
8. A.-M. Levelut, E. Hallouin, D. Bennemann, G. Heppke and D. Lötzsch, *J. Phys. II*, 1997, **7**, 981-1000.
9. T. Yamamoto, I. Nishiyama, M. Yoneya and H. Yokoyama, *J. Phys. Chem. B*, 2009, **113**, 11564-11567.
10. I. W. Hamley, J. P. Fairclough, A. J. Ryan, S.-M. Mai and C. Booth, *Phys. Chem. Chem. Phys.*, 1999, **1**, 2097-2101.
11. M. Impéror-Clerc, M. Veber and A. M. Levelut, *ChemPhysChem*, 2001, **2**, 533-535.
12. S. Kutsumizu, *Current opinion in solid state and materials science*, 2002, **6**, 537-543.
13. M. F. Schulz, F. S. Bates, K. Almdal and K. Mortensen, *Phys. Rev. Lett.*, 1994, **73**, 86-89.
14. T. Honda and T. Kawakatsu, *Macromolecules*, 2006, **39**, 2340-2349.
15. M. Nonomura, K. Yamada and T. Ohta, *J. Phys.: Condens. Matter*, 2003, **15**, L423.
16. Y. Huang, J. Yang, H. Cai, Y. Zhai, D. Feng, Y. Deng, B. Tu and D. Zhao, *J. Mater. Chem.*, 2009, **19**, 6536-6541.
17. L. Zhu, L. Sun, J. Miao, L. Cui, Q. Ge, R. P. Quirk, C. Xue, S. Z. Cheng, B. S. Hsiao and C. A. Avila-Orta, MRS Proceedings, 2004.
18. A. M. Squires, R. Templer, J. Seddon, J. Woenkhaus, R. Winter, T. Narayanan and S. Finet, *Phys. Rev. E*, 2005, **72**, 011502.
19. M. Yoneya, T. Yamamoto, I. Nishiyama and H. Yokoyama, *J. Phys. Chem. B*, 2008, **112**, 8452-8458.
20. G. E. Schröder-Turk, A. Fogden and S. T. Hyde, *Eur. Phys. J. B*, 2006, **54**, 509-524.
21. A. Fogden and S. T. Hyde, *Eur. Phys. J. B*, 1999, **7**, 91-104.
22. M. Clerc and E. Dubois-Violette, *J. Phys. II*, 1994, **4**, 275-286.
23. P. Harper, S. Gruner, R. Lewis and R. McElhaney, *Eur. Phys. J. E*, 2000, **2**, 229-245.
24. J. Enlow, R. Enlow, K. McGrath and M. Tate, |*J. Phys. Chem.*, 2004, **120**, 1981-1989.
25. P. Garstecki and R. Holyst, *Langmuir*, 2002, **18**, 2519-2528.
26. X. Zeng, G. Ungar and M. Impéror-Clerc, *Nature materials*, 2005, **4**, 562-567.
27. X. Zeng, L. Cseh, G. H. Mehl and G. Ungar, *J. Mater. Chem.*, 2008, **18**, 2953-2961.
28. K. Ozawa, Y. Yamamura, S. Yasuzuka, H. Mori, S. Kutsumizu and K. Saito, *J. Phys. Chem. B*, 2008, **112**, 12179-12181.
29. *International Tables for Crystallography*, Kluwer Academic Publishers, 1995.
30. P. Kekicheff and B. Cabane, *Acta Cryst. B*, 1988, **44**, 395-406.
31. B. Pansu, Y. Nastishin, M. Impéror-Clerc, M. Veber and H. Nguyen, *Eur. Phys. J. E*, 2004, **15**, 225-230.

TOC

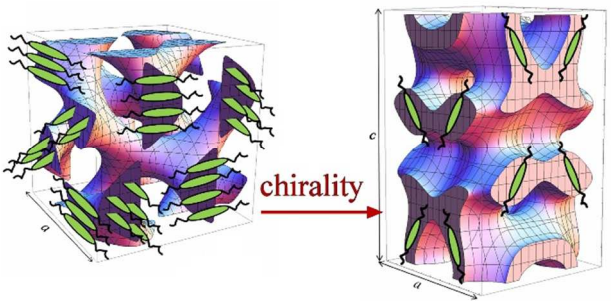

For rod-like molecules with two chiral centers de-racemization results in formation of a tetragonal mesophase instead of a cubic one.